DTIC FILE COPY

(2)

Naval Research Laboratory

Washington, DC 20375-5000

NRL Memorandum Report 6214

AD-A196 747

An Electron Ring Extraction Scheme from The Modified Betatron Accelerator

C. A. KAPETANAKOS

Plasma Physics Division

S. J. MARSH

Sachs/Freeman Associates, Inc.
Landover, MD 20785

D. DIALETIS

Science Applications, Inc.
McLean, VA 22102

June 27, 1988

SECURITY CLASSIFICATION OF THIS PAGE

REPORT DOCUMENTATION PAGE

1a. REPORT SECURITY CLASSIFICATION UNCLASSIFIED	1b. RESTRICTIVE MARKINGS
2a. SECURITY CLASSIFICATION AUTHORITY 2b. DECLASSIFICATION / DOWNGRADING SCHEDULE	3. DISTRIBUTION / AVAILABILITY OF REPORT Approved for public release; distribution unlimited.
4. PERFORMING ORGANIZATION REPORT NUMBER(S) NRL Memorandum Report 6214	5. MONITORING ORGANIZATION REPORT NUMBER(S)
6a. NAME OF PERFORMING ORGANIZATION Naval Research Laboratory 6b. OFFICE SYMBOL (If applicable) Code 4710	7a. NAME OF MONITORING ORGANIZATION
6c. ADDRESS (City, State, and ZIP Code) Washington, DC 20375-5000	7b. ADDRESS (City, State, and ZIP Code)
8a. NAME OF FUNDING / SPONSORING ORGANIZATION SPAWAR and ONR 8b. OFFICE SYMBOL (If applicable)	9. PROCUREMENT INSTRUMENT IDENTIFICATION NUMBER
8c. ADDRESS (City, State, and ZIP Code) Washington, DC 20362-5101	10. SOURCE OF FUNDING NUMBERS PROGRAM ELEMENT NO. 61153N PROJECT NO. N0003987 WRZ00209-41 TASK NO. WORK UNIT ACCESSION NO.

11. TITLE (Include Security Classification)
An Electron Ring Extraction Scheme From the Modified Betatron Accelerator

12. PERSONAL AUTHOR(S)
Kapetanakos, C.A., Marsh,* S.J. and Dialetis,** D.

13a. TYPE OF REPORT	13b. TIME COVERED	14. DATE OF REPORT (Year, Month, Day)	15. PAGE COUNT
Interim	FROM ____ TO ____	1988 June 27	36

16. SUPPLEMENTARY NOTATION
*Sachs/Freeman Associates, Inc., Landover MD 20785
**Science Applications, Inc., McLean, VA 22102

17. COSATI CODES			18. SUBJECT TERMS (Continue on reverse if necessary and identify by block number)
FIELD	GROUP	SUB-GROUP	Compact accelerators
			Modified betatron
			Extraction

19. ABSTRACT (Continue on reverse if necessary and identify by block number)

A technique is proposed for extracting the electron ring from the modified betatron accelerator. Basically, this technique consists of exciting the resonance that naturally exists for some specific values of the ratio of the vertical to toroidal magnetic field.

20. DISTRIBUTION / AVAILABILITY OF ABSTRACT ☒ UNCLASSIFIED/UNLIMITED ☐ SAME AS RPT. ☐ DTIC USERS	21. ABSTRACT SECURITY CLASSIFICATION UNCLASSIFIED
22a. NAME OF RESPONSIBLE INDIVIDUAL C.A. Kapetanakos	22b. TELEPHONE (Include Area Code) (202) 767-2838 22c. OFFICE SYMBOL Code 4710

DD FORM 1473, 84 MAR — 83 APR edition may be used until exhausted. All other editions are obsolete.

SECURITY CLASSIFICATION OF THIS PAGE

CONTENTS

AN ELECTRON RING EXTRACTION SCHEME FROM THE MODIFIED BETATRON ACCELERATOR

INTRODUCTION

The modified betatron accelerator[1,2] is one among the several compact[1-5] high current accelerator concepts currently under development in various laboratories. In this device a strong toroidal magnetic field B_θ has been added to the conventional betatron[6] magnetic field configuration. Although B_θ substantially improves the stability of the conventional betatron, the beam injection and capture and the electron ring extraction after the completion of acceleration are substantially more involved as a result of the toroidal field.

In this report, we describe on an extraction scheme that is easily realizable and has the potential to lead to very high extraction efficiency. Briefly, the proposed extraction scheme is based on the transformation of the circulating electron ring into a stationary helix, in the toroidal direction, by exciting the resonance that naturally exists for some specific values of the ratio of the vertical to toroidal magnetic field. Transformation of the ring into a helix is achieved with a localized vertical magnetic field disturbance that is generated by an agitator coil. As the minor radius of the helix increases with each passage through the gap of the agitator coil, the electrons eventually reach the extractor, which has the property that all the magnetic field components transverse to its axis are equal to zero. Thus, the electron ring unwinds into a straight beam.

Description of the Extraction Scheme

After the completion of acceleration, i.e., when the desired electron beam energy has been achieved, the electron ring centroid is displaced radially by intentionally mismatching the magnetic flux and the betatron magnetic field. In the results that

Manuscript approved March 21, 1988.

will be shown in the next Section, this mismatch has been achieved by superimposing a low amplitude vertical magnetic field that varies exponentially with time on the betatron field. It has been shown theoretically and verified by extensive numerical results that during the radial displacement of the ring centroid the amplitude of the slow mode[1] remains very small, i.e., a few mm, provided the mismatching field varies slowly with respect to the ring bounce (poloidal) period. Furthermore, computer simulations with the NRL MOBE particle-in-cell computer code have shown that during the radial displacement, that lasts several microseconds, the minor cross section of the ring preserves its integrity and the ring emittance remains constant.

As the major radius of the ring centroid increases slowly with time, the gyrating electrons reach the localized magnetic disturbance generated by the agitator coil. At this radial position the ratio of the vertical magnetic field B_z to the toroidal magnetic field B_θ has been selected to satisfy the condition

$$B_z/B_\theta = 2\,l/(2\,l^2-1), \qquad (1)$$

where $l = 1,2,3$ ......

Equation (1) implies that the frequency of the fast mode[1] is l times the frequency of gyration around the major axis. When $B_\theta >> B_z$, Eq. (1) is reduced to $\Omega_\theta = l\Omega_z$, where $\Omega_\theta = eB_\theta/m$ and $\Omega_z = eB_z/m$.

The purpose of the magnetic disturbance is to excite the resonance[7,8]. As an electron enters the lower magnetic field region of the disturbance, its velocity vector that initially is directed in the toroidal direction, rotates slightly in the radial direction, i.e., the electron obtains a radial velocity component. It can be shown from the equations of motion that this radial velocity is given by

$$\Delta v_r \simeq -2(\Delta\Omega_z^a/\gamma)r_a \; \Delta\theta, \qquad (2)$$

where $\Delta\Omega_z^a$ is the cyclotron frequency that corresponds to the field of the disturbance generated by the agitator coil, γ is the relativistic factor, r_a is the radial distance of the agitator coil and $\Delta\theta$ is the toroidal half width of the magnetic disturbance.

As a result of the acquired radial velocity, the electrons start to gyrate in the toroidal magnetic field with a radius

$$\rho = 2(N/l)(\Delta\Omega_z^a/\Omega_z) \; r_a \; \Delta\theta, \qquad (3)$$

where N is the number of passes through the disturbance. If condition (1) is not satisfied, ρ grows as $N^{1/2}$ instead of proportionally to N.

Since γ is very large, self fields can be ignored. However, because of the gradient of B_z the slow mode[1] (bounce motion) is still excited and the orbits of electrons in the transverse (r,z) plane precess very slowly. Therefore, for times short in comparison with the bounce period, i.e., for a few revolutions around the major axis, all the electrons of the ring perform coherent motion and a stationary helix, in the toroidal direction, is formed. A top view of the helix is shown in Fig. 1, for $l = 3$.

Ideally, the radial gradient of the magnetic disturbance should be extremely high, because otherwise the fast mode[1] is excited before the ring reaches the disturbance. In the computer runs of the next Section a disturbance with a satisfactorily sharp radial gradient is obtained by the single turn agitator coil shown in Fig. 2. The radial gradient of the disturbance is further improved with two single turn loops that are located at the edges of the gap. The radial profile of the B_z field is shown schematically in Fig. 3. In the computer runs, the magnetic field of the disturbance has been obtained from exact analytical expressions that are given in the Appendix.

With successive passes through the disturbance of the agitator the radial excursion of the orbit increases until the gyrating electrons reach the extractor, which is located at $\theta=0$ and at a slightly greater radial distance than the agitator coil. The results of the next section were obtained with a simple extractor consisting of two parallel plates with current flowing in opposite directions. These two plates have infinite extent in the z and semi-infinite extent in the y direction. The linear current density of the plates is adjusted to make the total B_z between the plates at $\theta=0$ equal to zero. The side of the extractor at $\theta=0$ is completely enclosedby the thin conducting foil. As a result the fringing fields are absent. The elect ons enter the extractor through this foil without any substantial energy loss. At the entrance of the extractor the vertical displacement of the electrons and their radial velocity are almost zero. However, they have a small vertical velocity.

In practice, this extractor can be realized by bending the two plates to form a torus. In order for the field to be uniform over a finite vertical distance, the cross section of each plate, after bending, should be D-shaped. In the results of the next Section, the orbit of the extracted beam is terminated after it propagates tens of cm inside the extractor. The reason is that the disturbance of the extractor ΔB_z^e is independent of y while the betatron field decreases with y. Thus, cancellation of the fields is not achieved over the entire length of the extractor. In practice exact cancellation of the two fields can be obtained by increasing the separation of the two plates as y increases.

In the previous discussions, we have assumed that the magnetic disturbance generated by the agitator coil is static. An alternate mode of operation is to expand the ring until it reaches the gap of the agitator coil and then to rapidly pulse the coil. Since the inductance of the agitator is typically only a few nH, short rise times, of the order of 1 nsec can be achieved with modest voltages. In the pulsed mode of operation the fraction of the ring that will be lost is approximately equal to the ratio: coil rise time/ period of gyration around the major axis.

Finally, it should be noticed that an ion channel[9] formed by a laser beam along the axis of the extractor may improve the extraction process and eliminate the need for an additional coil to cancel the component of B_θ that is transverse to the axis of the extractor or the need to completely cancel the B_z inside the extractor.

RESULTS

We have studied the proposed extraction scheme in both the static and pulsed mode for a range of parameters that are compatible with the NRL modified betatron accelerator. In this report we will present results from five runs, one in the pulsed mode and four in the static mode. The various parameters of the runs for $\gamma=40$ are listed in Table I and the parameters of the runs for $\gamma=400$ are listed in Table II. Since $\gamma>>1$, self and image field have been ignored and therefore the ring current is not a relevant parameter. Also at this high γ the beam minor diameter is expected to be only a few mm.

In the run 267, the pulsed agitator was turned-on after the ring's major radius became 121 cm. Figure 4a shows the radial excursion of a typical electron that was located at $\theta=0$ at the turn-on of agitator. After a single pass through the agitator the electron obtains enough radial excursion to enter the extractor and is extracted. Figure 4b shows that the electron at the distrubance obtains a transverse velocity approximately $2.8\times10^{-2}c$. Equation (2) predicts a $\Delta v_r = 2.7\times10^{-2}c$. In addition, the numerical results show that the electron gyrates around B_θ with a 1 cm radius, which is also the radius predicted by Eq. (3).

In the run 269, the electron started at $r=110$ cm and was moved radially by the mismatching field. The elapsed time from the minor axis to the agitator is ~4.5 μsec, that corresponds to an average radial velocity of $\sim2.2\times10^{6}$ cm/sec. The amplitude of the slow mode is less than 2 mm. Figure 5a shows the radial excursions of a typical electron in the r,θ plane and Fig. 5b shows a top view of its orbit. The electrons reach the extractor with a vertical displacement from the midplane that is only a few mm. For the reason given in the previous section, the run was terminated after the electron propagated ~30 cm inside the extractor.

In the runs 268, 270, and 272 the γ was increased to 400 with a corresponding increase in the value of magnetic fields. Results from run 268 are shown in Fig. 6. Figure 6a shows the radial excursions of the electron and Fig. 6b is a top view of its orbit, when the resonance condition is satisfied at $r=120$ cm. The coherence of the radial excursions is remarkable. We have found that this coherence is preserved even when Eq. (1) is not satisfied exactly, i.e., when the value of B_θ field is off a few percent. In run 270 the value of B_θ was reduced by 2% from its corresponding value in run 268. The results are shown in Fig. 7. Finally, by operating at $l=1$ or $l=2$ instead of at $l=3$, the value of B_θ can be substantially reduced. The results for $l=2$ are shown in Fig. 8.

In conclusion, we have developed a new extraction scheme that is practical and has the potential, since all the electrons of the ring perform coherent motion, to lead to a very high extraction efficiency.

ACKNOWLEDGEMENT

The authors are grateful to Prof. D. Kerst, Drs. Jeff Golden, R. Faehl and P. Sprangle for many illuminating discussions.

TABLE I

List of various parameters for the runs shown in Figs. 4 and 5

RUN #	267	266
Agitator's mode	Pulsed	Static
Relativistic factor γ	40	40
Major radius r_o (cm)	100	100
Vertical field at r_o (G)	649.9	649.9
Toroidal field at r_o (G)	-1921	-1971
Field index n	0.5	0.5
Resonance integer l	3	3
Amplitude of mismatching field (G)	---	60
Time constant of mismatching field (μsec)	---	10
Agitator's toroidal position	1.3Π	1.26Π
Agitator's toroidal width $2\Delta\theta$(rad)	0.05	0.066
Agitator's inner radius (cm)	120	120
Agitator's outer radius (cm)	122	124
Agitator's opening (cm)	1.0	2
Agitator's linear current density (kA/cm)	0.25	0.375
Agitator's field ΔB_z^a (G)	-300	-450
Extractor's opening toroidal position	0	0
Extractor's minimum inner radius (cm)	121.5	120.5
Extractor's minimum outer radius (cm)	125.5	124.5
Extractor's field ΔB_z^e (G)	-590.0	-590

TABLE II
List of various parameters for the runs shown in Figs. 6, 7, and 8

RUN #	268	270	272
Agitator's mode	Static	Static	Static
Relativistic factor γ	400	400	400
Major radius r_o (cm)	100	100	100
Vertical field at r_o (G)	6501	6501	6501
Toroidal field at r_o (G)	-19710	-19310	-11940
Field index n	0.5	0.5	0.5
Resonance integer l	3	3	2
Amplitude of mismatching field (G)	600	600	600
Time constant of mismatching field (μsec)	10	10	10
Agitator's toroidal position	1.26π	1.26π	0.94π
Agitator's toroidal width $2\Delta\theta$(rad)	0.066	0.066	0.066
Agitator's inner radius (cm)	120	120	120
Agitator's outer radius (cm)	124	124	124
Agitator's opening (cm)	2	2.0	2
Agitator's linear current density (kA/cm)	3.75	3.75	3.75
Agitator's field ΔB_z^a (G)	-4500	-4500	-4500
Extractor's opening toroidal position	0	0	0
Extractor's minimum inner radius (cm)	120.5	120.5	120.5
Extractor's minimum outer radius (cm)	124.5	124.5	124.5
Extractor's field ΔB_z^e (G)	-5900	-5900	-5900

REFERENCES

1. C. A. Kapetanakos, P. Sprangle, D. P. Chernin, S. J. Marsh, and I. Haber, Phys. Fluids, 26, (1983), 1634.

2. H. Ishizuka, G. Lindley, B. Mandelbaum, A. Fisher, and N. Rostoker, Phys. Rev. Letts., 53, 266 (1984).

3. S. Humphries, Jr. and L. K. Len, Proc. of 1987 IEEE Part. Accel. Conf., page 914.

4. V. Bailey, L. Schlitt, M. Tiefenbank, S. Putnam, A. Mondelli, D. Chernin, and J. Petello, Proc. of 1987 IEEE Part. Accel. Conf., page 920.

5. W. K. Tucker, S. L. Shope, and D. E. Hasti, Proc. of 1987 IEEE Part. Accel. Conf., page 957.

6. D. W. Kerst, Nature 157, 90 (1940).

7. D. Chernin and P. Sprangle, Part. Accel. 12, 101 (1982).

8. D. Dialetis, S. J. Marsh, and C. A. Kapetanakos, Part. Accel. 21, 227 (1987).

9. B. Hui and Y. Y. Lau, Phys. Rev. Letts., 53, 2024 (1984).

APPENDIX

The Anplied Fields

The purpose of this Appendix is to describe the various magnetic fields that were used in the numerical integration of the ring orbits.

Let the global cylindrical coordinates be (r,θ,z) and the global cartesian coordinates be (x,y,z), so that

$$x = r \cos \theta, \qquad (1a)$$

$$y = r \sin \theta. \qquad (1b)$$

The two clindrical components of the applied betatron field, that were used in the code are:

$$B_z = B_{zo} \left(\frac{r_o}{r}\right)^n , \qquad (2a)$$

$$B_r = -B_{zo}\, n \,\frac{z}{r} , \qquad (2b)$$

where r_o is the major radius and n is the field index.

In addition to the betatron field, a time dependent homogeneous magnetic fiel the mismatching field, is applied to shift the electron ring radially outward. The mismatching field is given by

$$B_z^{mis} = B_{zo}^{mis} \,(1-e^{-t/\tau}) , \qquad (3)$$

where τ is the time constant.

The applied toroidal magnetic field varies inverse proportionally to the radial distance, i.e.,

$$B_\theta = B_{\theta o} \frac{r_o}{r} . \qquad (4)$$

The extractor consists of two parallel plates with current flowing in opposite directions. These plates have infinite extent in the z and semi-infinite extent in the y-direction. A thin conducting foil completely encloses the extractor at $\theta=0$. The magnetic field inside the extractor is given by

$$B_z^{ext} = \frac{4\pi}{c} I_1^{ext} \quad , \tag{4}$$

where I_1^{ext} is the linear current density of the extractor.

Outside the extractor, the linear current density I_1^{ext} does not produce any field. The current of the extractor is adjusted to make the veritcal field zero near $\theta=0$.

The agitator field is more complicated. Let the agitator be located symmetrically at some toroidal angle θ_o, and let (x',y',z) be the local coordinate system of the agitator. Then

$$x' = x \cos \theta_o + y \sin \theta_o - r_1, \tag{5a}$$

$$y' = -x \sin \theta_o + y \cos \theta_o \quad , \tag{5b}$$

where r_1 is the radial distance of the minor axis of the agitator from the origin of the gloval coordinate system. In addition, let a be the radial width of the agitator, b its toroidal width and h the height of its gap. For simplicity, the toroidal correction will be omitted. In this case, the magnetic field of the agitator is that of a solenoid of rectangular cross section and infinite length minus the contribution of the missing piece of the solenoid of height h, radial length a, width b and linear current density I_1.

As a representative case, consider the contribution of one section of the missing piece of the solenoid, namely, the one which is perpendicular to the x'-axis and located at $x'=a/2$ in the local coordinate system of the agitator. The vector potential due to this section is equal to

$$A_{y'} = \frac{I_1}{c}\int_{-b/2}^{b/2} dy'' \int_{-h/2}^{h/2} dz'' \frac{1}{\left[\left(\frac{a}{2} - x'\right)^2 + \left(y''-y'\right)^2 + \left(z''-z\right)^2\right]^{1/2}} , \quad (6)$$

or, after performing the integral with respect to y",

$$A_{y'} = \frac{I_1}{c}\int_{-h/2}^{(h/2)} dz'' \ln \frac{\frac{b}{2} - y' + \left[\left(\frac{a}{2} - x'\right)^2 + \left(\frac{b}{2} - y'\right)^2 + \left(z''- z\right)^2\right]^{1/2}}{-\left(\frac{b}{2} + y'\right) + \left[\left(\frac{a}{2} - x'\right)^2 + \left(\frac{b}{2} + y'\right)^2 + \left(z''-z\right)^2\right]^{1/2}} \quad (7)$$

where Gaussian units are being used everywhere. The magnetic field is computed from the expressions

$$B_{x'} = -\frac{\partial A_{y'}}{\partial z} , \quad (8a)$$

$$B_z = \frac{\partial A_{y'}}{\partial x'} . \quad (8b)$$

The $B_{x'}$ - component is easily computed since $A_{y'}$ depends on z"- z, the $\partial/\partial z$ can be replaced by $-\partial/\partial z''$ inside the integral, and the integration with respect to z" becomes trivial. Therefore, we have

$$B_{x'} = \frac{I_1}{c}\left[\ln \frac{\frac{b}{2} - y' + \left[\left(\frac{a}{2} - x'\right)^2 + \left(\frac{b}{2} - y'\right)^2 + \left(\frac{h}{2} - z\right)^2\right]^{1/2}}{-\left(\frac{b}{2} + y'\right) + \left[\left(\frac{a}{2} - x'\right)^2 + \left(\frac{b}{2} + y'\right)^2 + \left(\frac{h}{2} - z\right)^2\right]^{1/2}}\right.$$

$$-\ln \frac{\frac{b}{2} - y' + \left[\left(\frac{a}{2} - x'\right)^2 + \left(\frac{b}{2} - y'\right)^2 + \left(\frac{h}{2} + z\right)^2\right]^{1/2}}{-\left(\frac{b}{2} + y'\right) + \left[\left(\frac{a}{2} - x'\right)^2 + \left(\frac{b}{2} + y'\right)^2 + \left(\frac{h}{2} + z\right)^2\right]^{1/2}} \Bigg] \quad . \tag{9}$$

In order to write the fields in compact form, we introduce the following functions:

$$h_p = \frac{h}{2} - z \quad , \tag{10a}$$

$$h_m = -\frac{h}{2} - z \quad , \tag{10b}$$

$$f_p^2 = u^2 + v_p^2 \quad , \tag{11a}$$

$$f_m^2 = u^2 + v_m^2 \quad , \tag{11b}$$

$$f_{pp}^2 = f_p^2 + h_p^2 \quad , \tag{12a}$$

$$f_{pm}^2 = f_p^2 + h_m^2 \quad , \tag{12b}$$

$$f_{mp}^2 = f_m^2 + h_p^2 \quad , \tag{12c}$$

$$f_{mm}^2 = f_m^2 + h_m^2 \quad , \tag{12d}$$

$$g_{pp} = v_p + f_{pp} \quad , \tag{13a}$$

$$g_{pm} = v_p + f_{pm} \quad , \tag{13b}$$

$$g_{mp} = v_m + f_{mp} \quad , \tag{13c}$$

$$g_{mm} = v_m + f_{mm} \quad . \tag{13d}$$

where the variables u, v_p, and v_m will be defined later on.

Furthermore, by defining the following two qualities

$$\hat{A}\,(u,\ v_p,\ v_m,\ Z,\ h) = \ln\left(\frac{g_{pp}\ g_{mm}}{g_{pm}\ g_{mp}}\right), \tag{14a}$$

$$\hat{B}\,(u,\ v_p,\ v_m,\ z,\ h) = \text{sign}\ (u) * $$

$$\left\{\text{sign}\ (h_p) * \text{Arcsin}\left(\frac{f_p^2 + v_p\ f_{pp}}{f_p\ g_{pp}}\right)\right.$$

$$- \text{sign}\ (h_p) * \text{Arcsin}\left(\frac{f_m^2 + v_m\ f_{mp}}{f_m\ g_{mp}}\right)$$

$$- \text{sign}\ (h_m) * \text{Arcsin}\left(\frac{f_p^2 + V_p\ f_{pm}}{f_p\ g_{pm}}\right)$$

$$\left. + \text{sign}\ (h_m) * \text{Arcsin}\left(\frac{f_m^2 + V_m\ f_{mm}}{f_m\ g_{mm}}\right)\right\}\quad, \tag{14b}$$

the $B_{x'}$ component can be written as

$$B_{x'}(x',\ y',\ z) = \frac{I_1}{c}\ \hat{A}\left(\frac{a}{2} - x',\ \frac{b}{2} - y',\ -\frac{b}{2} - y',\ z,\ h\right) \quad . \tag{15}$$

The B_z component is obtained from Equs. (8b) and (7) and is equal to

$$B_z = -\frac{I_1}{c}\int_{-h/2}^{h/2} dz'' \left[\frac{\frac{a}{2} - x'}{\left((z''-z)^2 + \left(\frac{a}{2} - x'\right)^2 + \left(\frac{b}{2} - y'\right)^2 + \left(\frac{b}{2} - y'\right)\right)\left[(z''-z)^2 + \left(\frac{a}{2} - x'\right)^2 + \left(\frac{b}{2} - y'\right)^2\right]^{1/2}}\right.$$

$$\left. - \frac{\frac{a}{2} - x'}{\left((z''-z)^2 + \left(\frac{a}{2} - x'\right)^2 + \left(\frac{b}{2} + y'\right)^2 - \left(\frac{b}{2} + y'\right)\right)\left[(z''-z)^2 + \left(\frac{a}{2} - x'\right)^2 + \left(\frac{b}{2} + y'\right)^2\right]^{1/2}}\right] \tag{16}$$

These are integrable functions and the B_z component can be expressed in terms of $\hat{B}$ as follows:

$$B_z(x',y',z) = \frac{I_1}{c}\, \hat{B}\left(\frac{a}{2} - x',\ \frac{b}{2} - y',\ -\frac{b}{2} - y',\ z,\ h\right) \quad . \qquad (17)$$

In a similar fashion, the contribution of the other three sections can be computed and the total contribution of all four sections of the missing piece is:

$$B_{x'}(x',\ y',\ z) = \frac{I_1}{c}\left[\hat{A}\left(\frac{a}{2} - x',\ \frac{b}{2} - y',\ -\frac{b}{2} - y',\ z,\ h\right) - \hat{A}\left(-\frac{a}{2} - x',\ \frac{b}{2} - y',\ -\frac{b}{2} - y',\ z,\ h\right)\right], \qquad (18a)$$

$$B_{y'}(x',\ y',\ z) = \frac{I_1}{c}\left[\hat{A}\left(\frac{b}{2} - y',\ \frac{a}{2} - x',\ -\frac{a}{2} - x',\ z,\ h\right) - \hat{A}\left(-\frac{b}{2} - y',\ \frac{a}{2} - x',\ -\frac{a}{2} - x',\ z,\ h\right)\right], \qquad (18b)$$

$$\begin{aligned} B_z(x',\ y'\ z) = \frac{I_1}{c}\Bigg[& \hat{B}\left(\frac{a}{2} - x',\ \frac{b}{2} - y',\ -\frac{b}{2} - y',\ z,\ h\right) \\ & - \hat{B}\left(-\frac{a}{2} - x',\ \frac{b}{2} - y',\ -\frac{b}{2} - y',\ z,\ h\right) \\ & + \hat{B}\left(\frac{b}{2} - y',\ \frac{a}{2} - x',\ -\frac{a}{2} - x',\ z,\ h\right) \\ & - \hat{B}\left(-\frac{b}{2} - y',\ \frac{a}{2} - x',\ -\frac{a}{2} - x',\ z,\ h\right)\Bigg] . \end{aligned} \qquad (18c)$$

As mentioned above, these fields should be subtracted from the magnetic field of the solenoid, which is equal to

$$B_z = \begin{cases} \frac{4\pi}{c} I_1 & \text{inside the solenoid} \\ 0 & \text{outside the solenoid.} \end{cases} \tag{19}$$

In the order to make the fields drop sharper in the radial direction, two rectangular loops at $z = h/z$ and $z = -h/2$ were added to the agitator, to compensate for the missing current of the gap. The radial and the toroidal width of the loops were the same as those of the rectangular solenoid, while the current in each loop was chosen equal to

$$I_w = - \frac{I_1 h}{2} \quad . \tag{20}$$

The computation of the magnetic fields of these two loops is straight forward. It is convenient to define the following two functions:

$$\hat{A}_w(u, v_p, v_m, z, h) =$$

$$= h_p \left(\frac{1}{f_{pp}\, g_{pp}} - \frac{1}{f_{mp}\, g_{mp}}\right)$$

$$- h_m \left(\frac{1}{f_{pm}\, g_{pm}} - \frac{1}{f_{mm}\, g_{mm}}\right) \quad , \tag{21a}$$

$$\hat{B}_w (u, v_p, v_m, z, h) = \tag{21b}$$

$$= - u \left(\frac{1}{f_{pp}\, g_{pp}} - \frac{1}{f_{mp}\, g_{mp}} + \frac{1}{f_{pm}\, g_{pm}} - \frac{1}{f_{mm}\, g_{mm}}\right) ,$$

where all quantities have already been defined in Eqs. (10) - (13). Then the magnetic field components of both loops are:

$$B_{x'}^{(w)}(x', y', z) = \frac{I_w}{c}\left[\hat{A}_w\left(\frac{a}{2} - x', \frac{b}{2} - y', -\frac{b}{2} - y', z, h\right)\right.$$

$$\left. - \hat{A}_w\left(-\frac{a}{2} - x', \frac{b}{2} - y', -\frac{b}{2} - y', z, h\right)\right] \qquad (22a)$$

$$B_{y'}^{(w)}(x', y', z) = \frac{I_w}{c}\left[\hat{A}_w\left(\frac{b}{2} - y', \frac{a}{2} - x', -\frac{a}{2} - x', z, h\right)\right.$$

$$\left. - \hat{A}_w\left(-\frac{b}{2} - y', \frac{a}{2} - x', -\frac{a}{2} - x', z, h\right)\right], \qquad (22b)$$

$$B_{z}^{(w)}(x', y', z) = \frac{I_w}{c}\left[\hat{B}_w\left(\frac{a}{2} - x', \frac{b}{2} - y', -\frac{b}{2} - y', z, h\right)\right.$$

$$- \hat{B}_w\left(-\frac{a}{2} - x', \frac{b}{2} - y', -\frac{b}{2} - y', z, h\right)$$

$$+ \hat{B}_w\left(\frac{b}{2} - y', \frac{a}{2} - x', -\frac{a}{2} - x', z, h\right)$$

$$\left. - \hat{B}_w\left(-\frac{b}{2} - y', \frac{a}{2} - x', -\frac{a}{2} - x', z, h\right)\right]. \qquad (22c)$$

These components are easily transformed from the local coordinate system of the agitator to the global coordinate system.

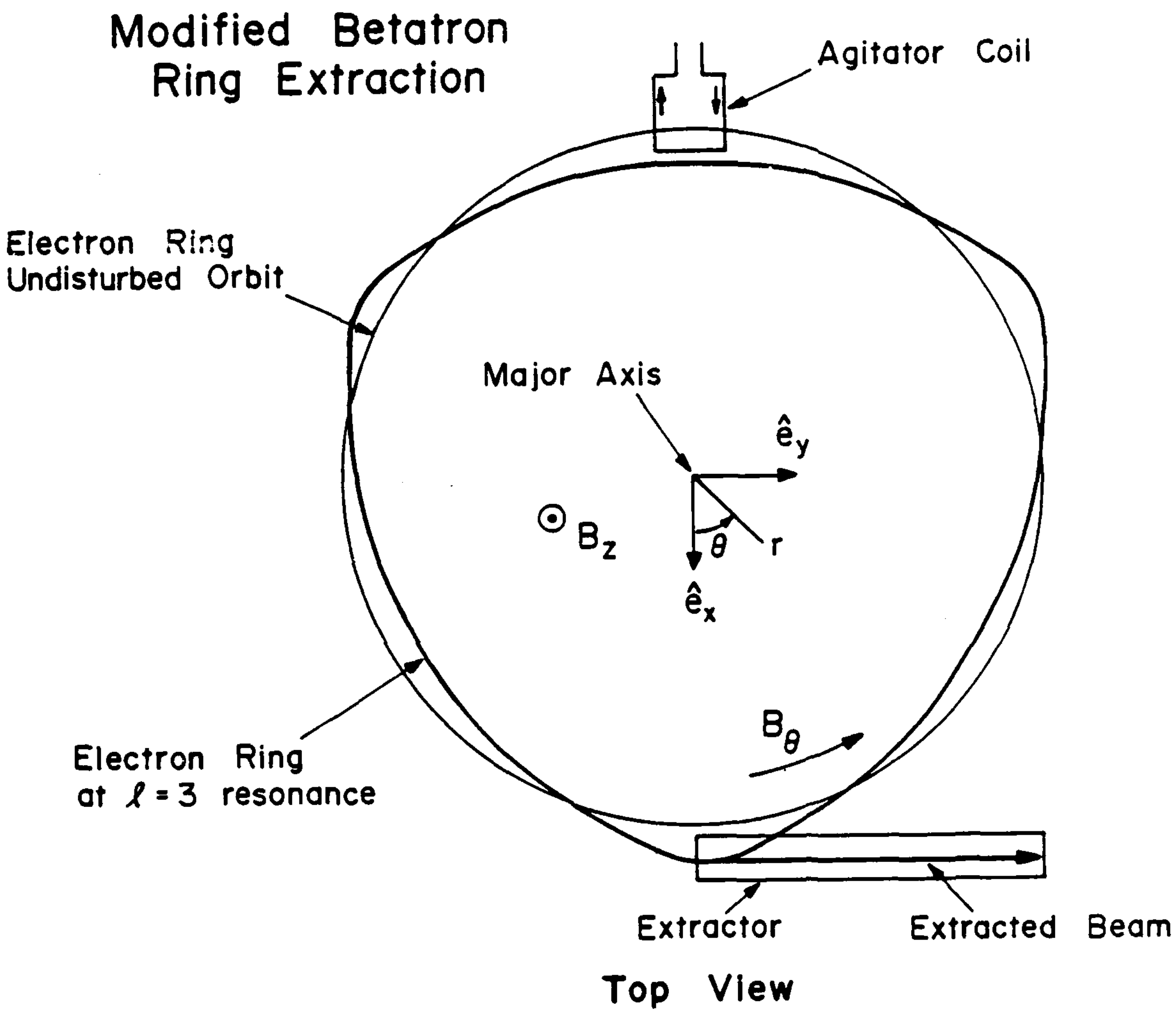

Fig. 1. Schematic of the proposed extraction scheme.

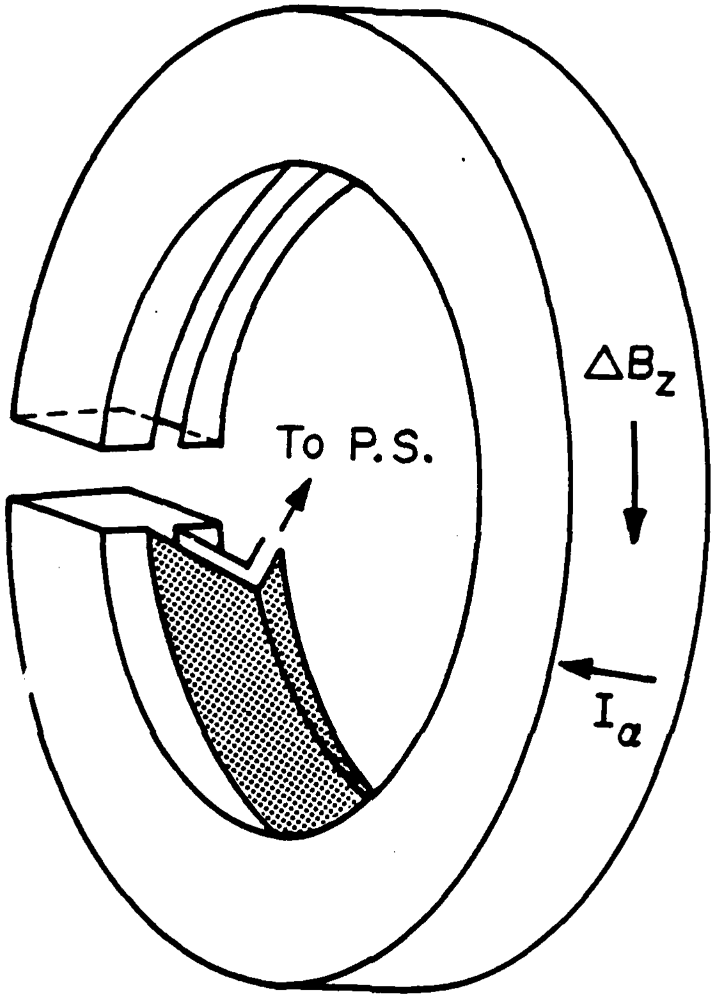

Agitator Coil

Fig. 2. Agitator coil that generates the localized disturbance. It is powered by a coaxial transmission line.

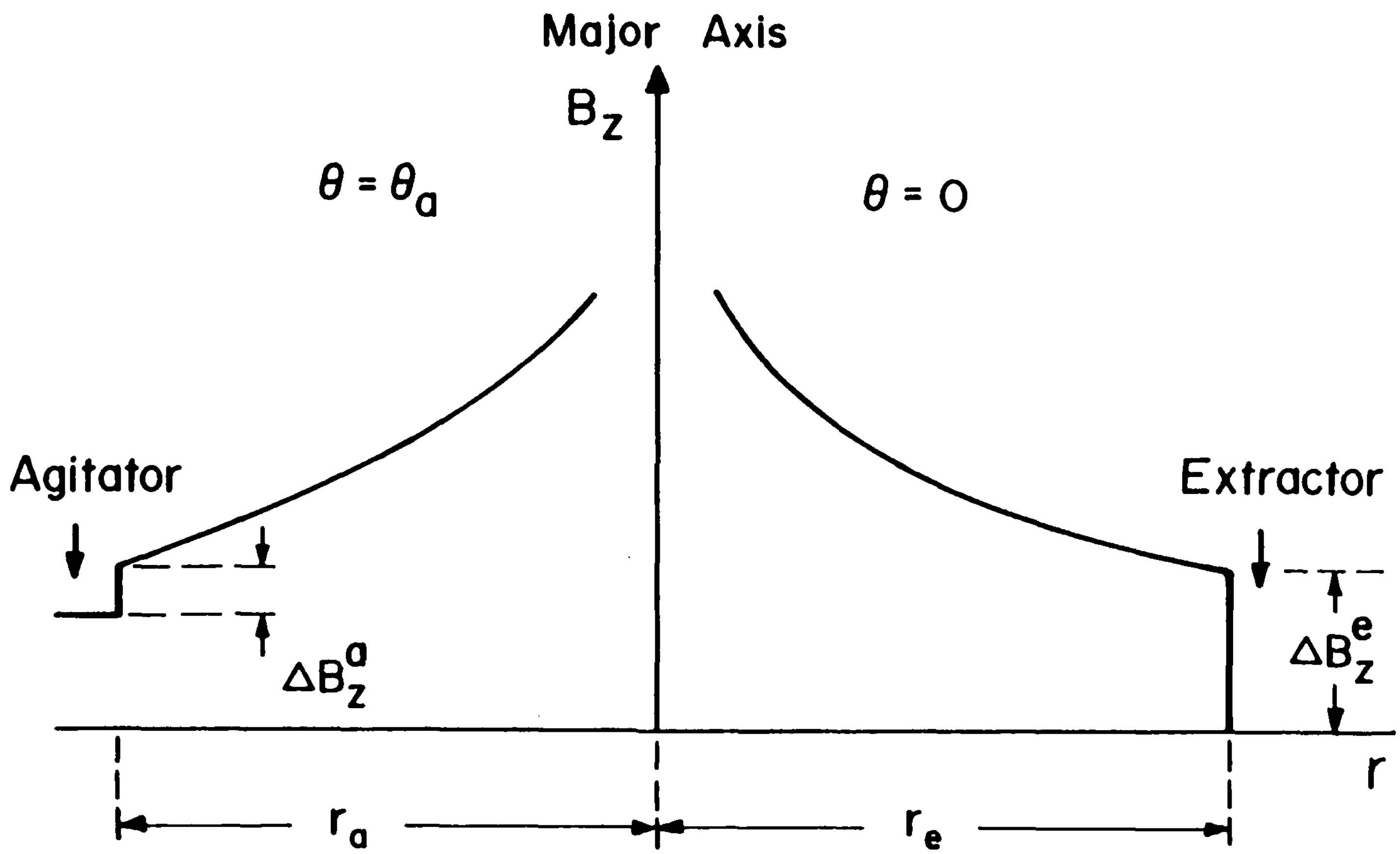

Fig. 3. Radial profile of the vertical magnetic field.

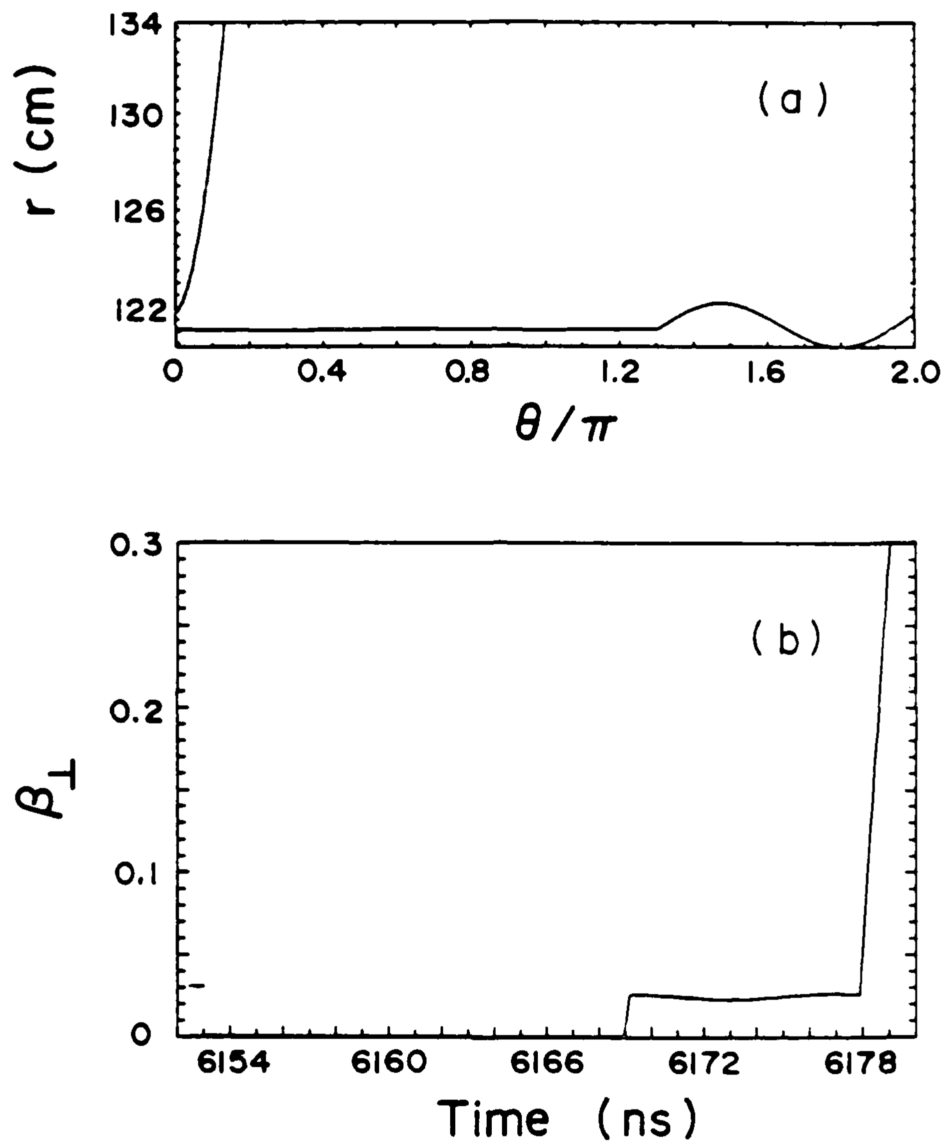

Fig. 4. Radial excursions of a typical electron (1) and its corresponding normalized transverse velocity (b) for the run 267.

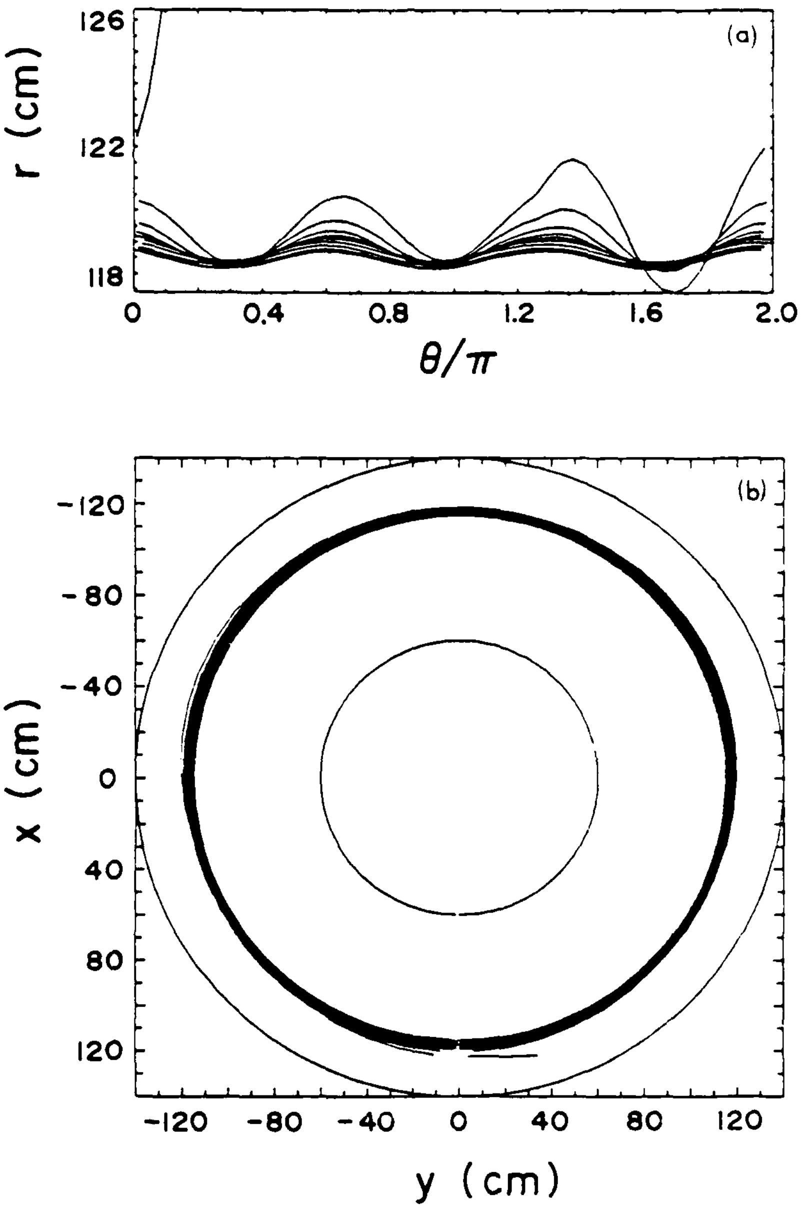

Fig. 5. Radial excursions of a typical electron (a) and top view of its trajectory in the x,y plane for the run 266.

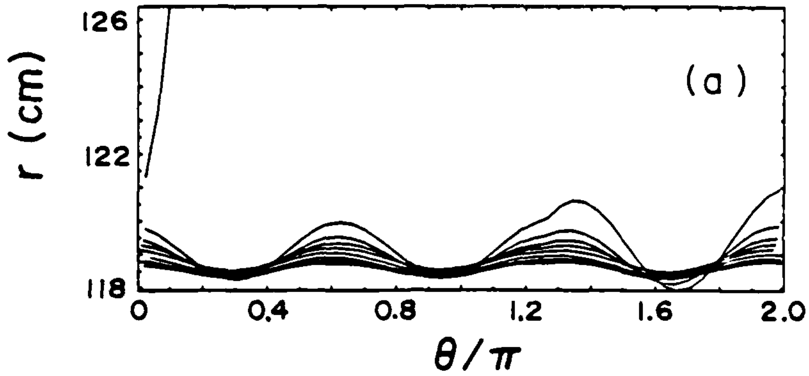

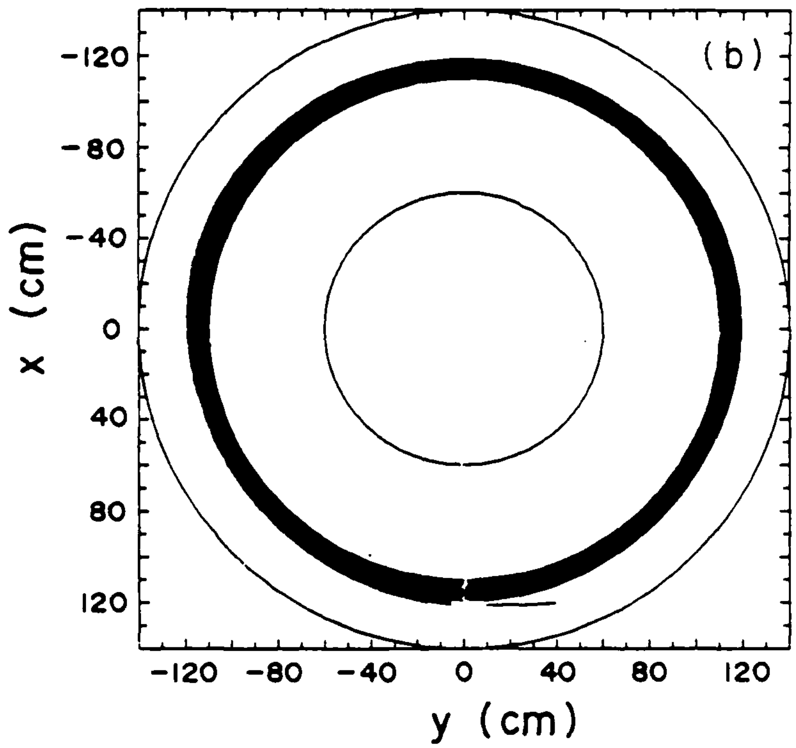

Fig. 6. Radial excursion of a typical electron (a) and top view of its trajectory in the the x,y plane for the run 268.

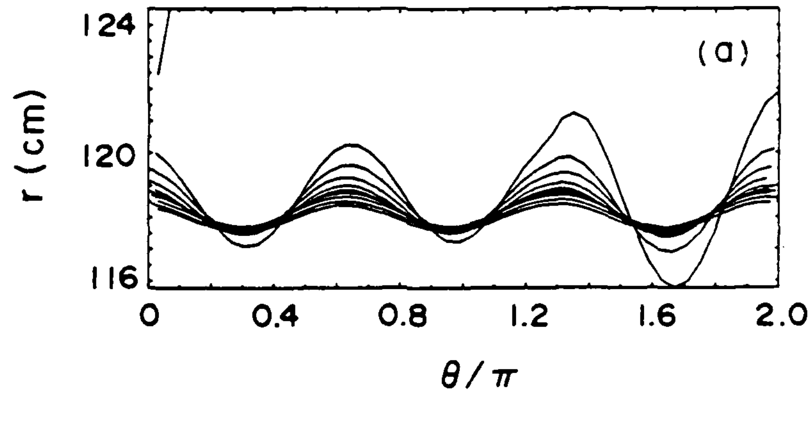

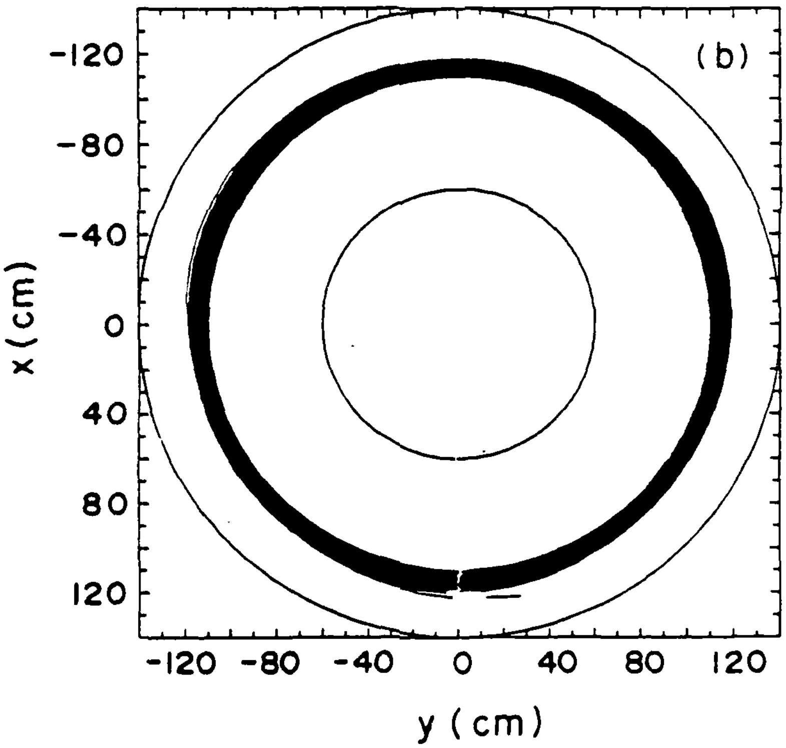

Fig. 7. Radial excursion of a typical electron (a) and top view of its trajectory in the x,y plane for the run 270.

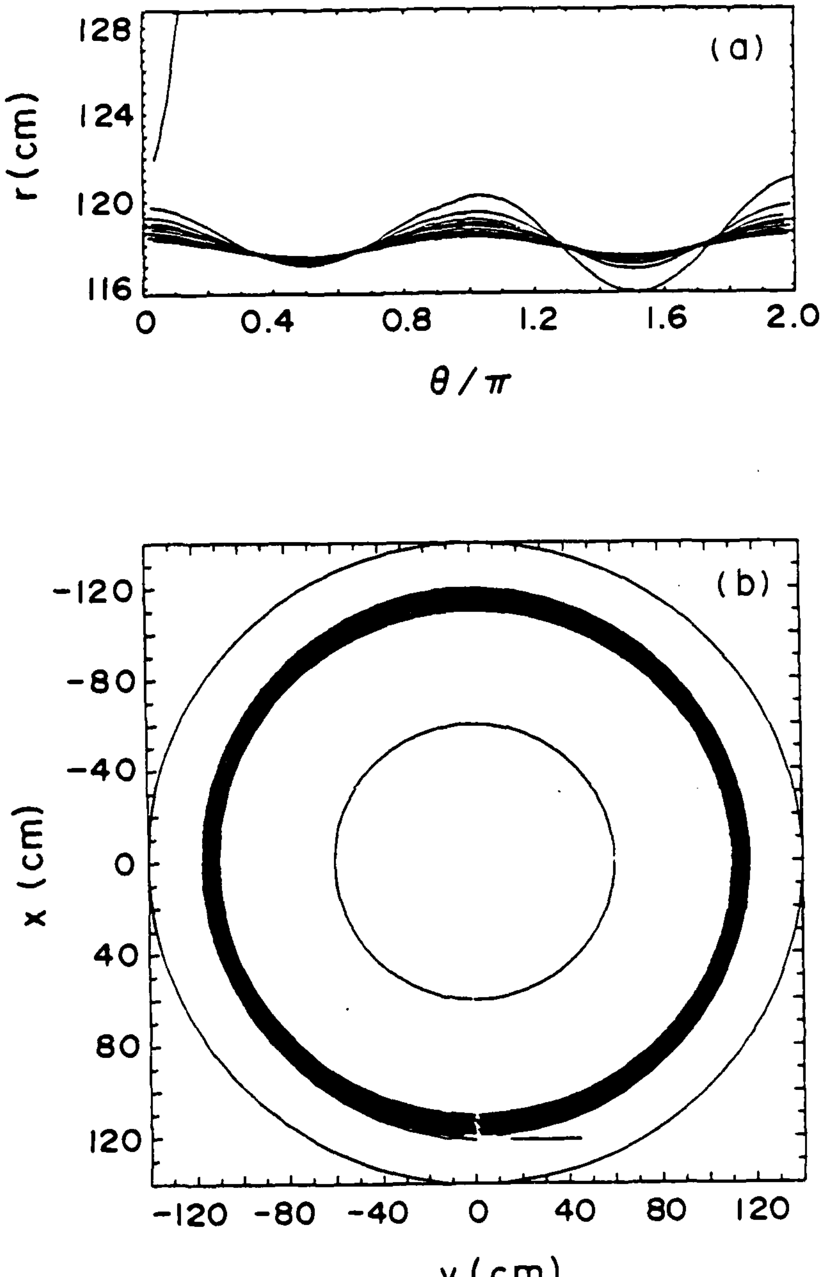

Fig. 8. Radial excursion of a typical electron (a) and top view of its trajectory in the x,y plane for the run 272.

DISTRIBUTION LIST
(Revised December 31, 1987)

Dr. M. Allen
Stanford Linear Accelerator Center
Stanford, CA 94305

Dr. V. Barletta
Lawrence Livermore National Laboratory
P.O. Box 808
Livermore, CA 94550

Dr. M. Barton
Brookhaven National Laboratory
Upton, L.I., NY 11101

CDR William F. Bassett
APM for Test Systems Engineering
Naval Sea Systems Command, Code PMS-405
Washington, DC 20362-5101

Dr. Jim Benford
Physics International Co.
2700 Merced St.
San Leandro, CA 94577

Dr. Kenneth Bergerson
Plasma Theory Division - 5241
Sandia National Laboratories
Albuquerque, NM 87115

Dr. Daniel Birx
Lawrence Livermore National Laboratory
P.O. Box 808
Livermore, CA 94550

Dr. Charles Brau
Los Alamos Scientific Laboratory
Los Alamos, NM 87544

Dr. R. Briggs
Lawrence Livermore National Laboratory
P.O. Box 808
Livermore, CA 94550

Dr. Allan Bromborsky
Harry Diamond Laboratory
2800 Powder Mill Road
Adelphi, MD 20783

Dr. H. Lee Buchanan
DARPA
1400 Wilson Blvd.
Arlington, VA 22209-2308

Dr. M. Butram
Sandia National Laboratory
Albuquerque, NM 87115

Dr. M. Caponi
TRW Advance Tech. Lab.
I Space Park
Redondo Beach, CA 90278

Prof. F. Chen
Department of Electrical Engineering
University of California at Los Angeles
Los Angeles, CA 90024

Dr. D. Chernin
Science Applications Intl. Corp.
1710 Goodridge Drive
McLean, VA 22102

Dr. Charles C. Damm
Lawrence Livermore National Laboratory
P.O. Box 808
Livermore, CA 94550

Prof. R. Davidson
Plasma Fusion Center
M.I.T.
Cambridge, MA 02139

Dr. J. Dawson
University of California at Los Angeles
Department of Physics
Los Angeles, CA 90024

Dr. W.N. Destler
Department of Electrical Engineering
University of Maryland
College Park, MD 20742

Prof. W. Doggett
North Carolina State University
P.O. Box 5342
Raleigh, NC 27650

Dr. H. Dreicer
Director Plasma Physics Division
Los Alamos Scientific Laboratory
Los Alamos, NM 87544

Prof. W.E. Drummond
Austin Research Associates
1901 Rutland Drive
Austin, TX 78758

Dr. Don Eccleshall
Bldg. 120-Room 241
Ballistic Research Lab.
Aberdeen Proving Grounds
Aberdeen, MD 21005

Dr. J.G. Eden
Department of Electrical Engineering
University of Illinois
155 EEB
Urbana, IL 61801

Dr. A. Faltens
Lawrence Berkeley Laboratory
Berkeley, CA 94720

Dr. T. Fessenden
Lawrence Livermore National Laboratory
P.O. Box 808
Livermore, CA 94550

Dr. A. Fisher
Physics Department
University of California
Irvine, CA 92664

Prof. H.H. Fleischmann
Laboratory for Plasma Studies and
School of Applied and Eng. Physics
Cornell University
Ithaca, NY 14850

Dr. T. Fowler
Associate Director
Magnetic Fusion Energy
Lawrence Livermore National Laboratory
P.O. Box 808
Livermore, CA 94550

Mr. George B. Frazier, Manager
Pulsed Power Research & Engineering Dept.
2700 Merced St.
P.O. Box 1538
San Leandro, CA 94577

LCDR W. Fritchie
APM for Test Systems Engineering
Naval Sea Systems Command, Code PMS-405
Washington, DC 20362-5101

Dr. S. Graybill
Harry Diamond Laboratory
2800 Powder Mill Road
Adelphi, MD 20783

Lt. Col. R. Gullickson
SDIO-DEO
Pentagon
Washington, DC 20301-7100

Dr. Z.G.T. Guiragossian
TRW Systems and Energy RI/1070
Advanced Technology Lab
1 Space Park
Redondo Beach, CA 90278

Prof. D. Hammer
Laboratory of Plasma Physics
Cornell University
Ithaca, NY 14850

Dr. David Hasti
Sandia National Laboratory
Albuquerque, NM 87115

Dr. C.E. Hollandsworth
Ballistic Research Laboratory
DRDAB - BLB
Aberdeen Proving Ground, MD 21005

Dr. C.M. Huddleston
ORI
1375 Piccard Drive
Rockville, MD 20850

Dr. S. Humphries
University of New Mexico
Albuquerque, NM 87131

Dr. Robert Hunter
9555 Distribution Ave.
Western Research Inc.
San Diego, CA 92121

Dr. J. Hyman
Hughes Research Laboratory
3011 Malibu Canyon Road
Malibu, CA 90265

Prof. H. Ishizuka
Department of Physics
University of California at Irvine
Irvine, CA 92664

Dr. D. Keefe
Lawrence Berkeley Laboratory
Building 50, Rm. 149
One Cyclotron Road
Berkely, CA 94720

Dr. Donald Kerst
University of Wisconsin
Madison, WI 53706

Dr. Edward Knapp
Los Alamos Scientific Laboratory
Los Alamos, NM 87544

Dr. A. Kolb
Maxwell Laboratories
8835 Balboa Ave.
San Diego, CA 92123

Dr. Peter Korn
Maxwell Laboratories
8835 Balboa Ave.
San Diego, CA 92123

Dr. R. Linford
Los Alamos Scientific Laboratory
P.O. Box 1663
Los Alamos, NM 87545

Dr. C.S. Liu
Department of Physics
University of Maryland
College Park, MD

Prof. R.V. Lovelace
School of Applied and Eng. Physics
Cornell University
Ithaca, NY 14853

Dr. S.C. Luckhardt
Plasma Fusion Center
M.I.T.
Cambridge, MA 02139

Dr. John Madey
Physics Department
Stanford University
Stanford, CA 94305

Dr. J.E. Maenchen
Division 1241
Sandia National Lab.
Albuquerque, NM 87511

Prof. T. Marshall
School of Engineering and Applied Science
Plasma Laboratory
S.W. Mudd Bldg.
Columbia University
New York, NY 10027

Dr. M. Mazarakis
Sandia National Laboratory
Albuquerque, NM 87115

Dr. D.A. McArthur
Sandia National Laboratories
Albuquerque, NM 87115

Prof. J.E. McCune
Dept. of Aero. and Astronomy
M.I.T.
77 Massachusetts Ave.
Cambridge, MA 02139

Prof. G.H. Miley, Chairman
Nuclear Engineering Program
214 Nuclear Engineering Lab.
Urbana, IL 61801

Dr. Bruce Miller
TITAN Systems
9191 Town Centre Dr.
Suite 500
San Diego, CA 92122

Dr. A. Mondelli
Science Applications, Inc.
1710 Goodridge Drive
McLean, VA 22102

Dr. Phillip Morton
Stanford Linear Accelerator Center
Stanford, CA 94305

Dr. M. Nahemow
Westinghouse Electric Corporation
1310 Beutah Rd.
Pittsburg, PA 15235

Prof. J. Nation
Lab. of Plasma Studies
Cornell University
Ithaca, NY 14850

Dr. V.K. Neil
Lawrence Livermore National Laboratory
P.O. Box 808
Livermore, CA 94550

Dr. Gene Nolting
Naval Surface Weapons Center
White Oak Laboratory
10901 New Hampshire Ave.
Silver Spring, MD 20903-5000

Dr. C.L. Olson
Sandia Laboratory
Albuquerque, NM 87115

Dr. Arthur Paul
Lawrence Livermore National Laboratory
P.O. Box 808
Livermore, CA 94550

Dr. S. Penner
National Bureau of Standards
Washington, D.C. 20234

Dr. Jack M. Peterson
Lawrence Berkeley Laboratory
Berkeley, CA 94720

Dr. R. Post
Lawrence Livermore National Lab.
P.O. Box 808
Livermore, CA 94550

Dr. Kenneth Prestwich
Sandia National Laboratory
Albuquerque, NM 87115

Dr. S. Prono
Lawrence Livermore National Lab.
P.O. Box 808
Livermore, CA 94550

Dr. Sid Putnam
Pulse Science, Inc.
600 McCormick Street
San Leandro, CA 94577

Dr. Louis L. Reginato
Lawrence Livermore National Lab
P.O. Box 808
Livermore, CA 94550

Prof. N. Reiser
Dept. of Physics and Astronomy
University of Maryland
College Park, MD 20742

Dr. M.E. Rensink
Lawrence Livermore National Lab
P.O. Box 808
Livermore, CA 94550

Dr. D. Rej
Lab for Plasma Physics
Cornell University
Ithaca, NY 14853

Dr. J.A. Rome
Oak Ridge National Lab
Oak Ridge, TN 37850

Prof. Norman Rostoker
Dept. of Physics
University of California
Irvine, CA 92664

Prof. George Schmidt
Physics Department
Stevens Institute of Tech.
Hoboken, NJ 07030

Philip E. Serafim
Northeastern University
Boston, MA 02115

Dr. Andrew Sessler
Lawrence Berkeley National Lab
Berkeley, CA 94720

Dr. John Siambis
Lockheed
Palo Alto Research Lab
3257 Hanover Street
Palo Alto, CA 94304

Dr. Adrian C. Smith
Lawrence Livermore National Laboratory
P.O. Box 808
Livermore, CA 94550

Dr. Lloyd Smith
Lawrence Berkeley National Laboratory
Berkeley, CA 94720

Dr. A. Sternlieb
Lawrence Berkely National Laboratory
Berkeley, CA 94720

Dr. D. Straw
W.J. Schafer Assoc.
2000 Randolph Road, S.E., Suite A
Albuquerque, NM 87106

Records 1 copy

Prof. C. Striffler
Dept. of Electrical Engineering
University of Maryland
College Park, MD 20742

Prof. R. Sudan
Laboratory of Plasma Studies
Cornell University
Ithaca, NY 14850

Dr. W. Tucker
Sandia National Laboratory
Albuquerque, NM 87115

Dr. H. Uhm
Naval Surface Weapons Center
White Oak Laboratory
10901 New Hampshire Ave. Code R41
Silver Spring, MD 20903-5000

Dr. William Weldon
University of Texas
Austin, TX 78758

Dr. Mark Wilson
National Bureau of Standards
Washington, DC 20234

Dr. P. Wilson
Stanford Linear Accelerator Center
Stanford, CA 94305

Prof. C.B. Wharton
303 N. Sunset Drive
Ithaca, NY 14850

Dr. Gerald Yonas
TITAN Systems
9191 Town Centre Drive
Suite 500
San Diego, CA 92122

West Defense Technical Information Center
- 2 copies

NRL Code 2628 - 20 copies

NRL Code 4700 - 26 copies

NRL Code 4710 - 40 copies

DIRECTOR OF RESEARCH
U.S. NAVAL ACADEMY
ANNAPOLIS, MD 21402
2 COPIES

CODE 1220
1 COPY

MAILING LIST/FOREIGN

Library
Institut fur Plasmaforschung
Universitat Stuttgart
Pfaffenwaldring 31
7000 Stuttgart 80, West Germany

Ken Takayama
KEN, TRISTAN Division
Oho, Tsukuba, Ibaraki, 305 JAPAN